Powder Technology 324 (2018) 62–68

Contents lists available at ScienceDirect

Powder Technology

journal homepage: www.elsevier.com/locate/powtec

One-step solvent-free mechanochemical synthesis of metal iodate fine powders

Haiyang Wang, Jeffery B. DeLisio, Tao Wu, Xizheng Wang, Michael R. Zachariah *

Department of Chemical and Biomolecular Engineering and Department of Chemistry and Biochemistry, University of Maryland, College Park, MD 20742, United States

ARTICLE INFO

Article history:
Received 23 June 2017
Received in revised form 2 October 2017
Accepted 8 October 2017
Available online 14 October 2017

Keywords:
Mechanochemical synthesis
Metal iodate
Solid-state
Superfine powders
Solvent-free

ABSTRACT

Metal iodates are strong iodine rich oxidizers which can be used in the formulation of biocidal energetic materials. Generally, metal iodates particles were synthesized by chemical precipitation methods with a large size distribution. In this work, we developed a one-step and solvent-free, high yield method to synthesize metal iodate fine powders by mechanochemistry. Compared to the conventional chemical precipitation method, the size of final products can be reduced by 20–500 times. The method generates particles with a narrower size distribution and high yield, and is sufficiently generic as to enable creation of a variety of metal iodates including $AgIO_3$, $Ca(IO_3)_2$, $Mn(IO_3)_2$ and $Cu(IO_3)_2$. Moreover, the synthesis is conducted in the solid states with little to no solvent. The role of process conditions (temperature, hydration state, and milling time) on reaction products was investigated by TG/DSC and XRD. We believe that crystalline water bound to the metal nitrates precursor lowers the Tammann's temperature sufficient to unbind water so as to promote ion diffusion and thus facilitate reaction in the absence of a solvent. The reaction is promoted by the milling process which attrits the particles to expose fresh unreacted surfaces and reduces particle size.

© 2017 Published by Elsevier B.V.

1. Introduction

"Mechanochemistry" refers to a technique that uses mechanical energy to induce physicochemical transformations and chemical reactions between solids [1–4]. So called "Green Manufacturing" approaches hope to minimize the use of solvents, particularly those that are petroleum based [2]. Mechanochemistry, particularly if conducted in a dry state offers the potential to significantly decrease the environmental footprint, from both an energy and chemical usage and disposal [1,2]. In recent years, mechanochemical techniques have evolved into a mainstream synthesis technique to produce various materials including inorganic solids [5,6], cocrystals [7], organics [8], and metal-organic frameworks (MOFs) [9]. In a mechanochemical process, chemical reactions occur at the interfaces of nanoscale layers that are continuously re-generated owing to repeated welding, deformation and fracture of the reactants mixture [10]. As a result, the temperature for inducing a chemical reaction in a mechanochemical process is lowered [10–15].

In this study, we focus on energetic material components that can be used in the neutralization of bacterial spores. Among different energetic systems, one of the most interesting are nanothermites, also known as metastable interstitial composites (MICs), consisting of nanosized fuel (normally aluminum nanoparticles, Al NPs) and nanosized metal oxides (such as CuO, Bi_2O_3, and Fe_2O_3), and shown to have >1000× higher reactivity when compared to conventional thermites [16–20]. Many techniques such as electrospray/electrospinning [21] and ball milling [22–24] (top-down), magnetron sputtering [25] and electrodeposition [26] (down-top), spray pyrolysis [27–29], precipitation [30,31] and combustion synthesis [32], etc. have been employed to generate the nanosized oxidizers in nanothermite systems. Using these methods, nanoparticles of various sizes and morphologies can be created. However, none of these methods simultaneously possess the three important characteristics for green manufacturing: solvent-free; low thermal budget, economical large-scale production.

Compared to metal oxides, metal iodates are much stronger oxidizers in thermite applications because upon decomposition, not only is corresponding metal oxides formed, by oxygen and iodine gas are released at relatively low temperatures [30,31,33]. One very important aspect of this is that one of the by-products of reaction elemental iodine, is a very effective biocide [23,27,29,31,33]. The large exothermicity from reactions with metals such as aluminum and the large iodine content make metal iodates viable candidates for neutralization of biological warfare agents such as *Bacillus anthracis* (anthrax) spores [30,31,33]. Table 1 shows data of iodine content, energy density and adiabatic flame temperatures for different metal iodates based thermites (determined by NASA CEA and Cheetah codes). As shown in Table 1, metal iodate based thermites (with aluminum) have relatively high iodine content (>40 wt%), high energy densities (~5 kJ/g) and high adiabatic flame temperatures (~4000 K). Commonly, metal iodates particles such as $AgIO_3$, $Ca(IO_3)_2$, $Mn(IO_3)_2$ and $Cu(IO_3)_2$ are synthesized by

Abbreviations: XRD, X-ray diffractometer; SEM, scanning electron microscope; EDS, Energy-dispersive X-ray spectroscopy; DI water, deionized water; Tm, melting point.

* Corresponding author.
E-mail address: mrz@umd.edu (M.R. Zachariah).

https://doi.org/10.1016/j.powtec.2017.10.024
0032-5910/© 2017 Published by Elsevier B.V.

Table 1
Iodine content, reaction heat and adiabatic flame temperature (AFT) of various metal iodates-based thermites.

Thermites	Iodine content (wt%)[a]	Reaction heat (kJ/g)[b]	AFT (K)[c]
$AgIO_3$ + 2Al	37.7	−3.89	3681[1, 7, 8]
$Bi(IO_3)_3$ + 6Al	42.5	−4.13	4062
$Cu(IO_3)_2$ + 4Al	48.7	−4.98	4061
$Fe(IO_3)_3$ + 6Al	51.3	−4.97	4043
$Mn(IO_3)_2$ + 4Al	49.5	−4.48	3971
$Ca(IO_3)_2$ + 4Al	51.0	−3.98	3909
CuO + (2/3) Al	0	−1.26	3054

[a] Based on stoichiometric ratio of the fuel and oxidizer.
[b] Calculated via www.materialsproject.org.
[c] Calculated by Cheetah codes except Al/$AgIO_3$, which is calculated by NASA CEA.

chemical precipitation methods which result in large particle size distributions. There are for example no superfine metal iodates commercially available [34]. However, smaller metal iodates particles are desired for high reactivity when formulated with nano aluminum. Previously, our group synthesized $AgIO_3$ sheets by a chemical precipitation method, but these produced a wide range of ~100 nm to 10 μm of $AgIO_3$ sheets [35,36]. Dreizin's group prepared B-$Ca(IO_3)_2$/Al-$Ca(IO_3)_2$ composites using commercial $Ca(IO_3)_2$, but were able to decrease the particle size to ~1 μm by arrested reactive milling [37,38]. In this paper, various superfine metal iodate particles were efficiently produced by simply milling the corresponding metal nitrates and potassium iodate with production yields >75%, with little to no solvent. Furthermore, the synthesized metal iodate particles are nanosized or submicron.

2. Experimental section

2.1. Chemicals

Copper (II) nitrate trihydrate (99.5%) was purchased from Strem Chemicals. Calcium (II) nitrate tetrahydrate (≥99.0%), manganese (II) nitrate tetrahydrate (≥97.0%), silver nitrate (≥99.0%), bismuth nitrate pentahydrate (≥98.0%), ferric nitrate nonahydrate (99.1%) and potassium iodate (99.5%) were purchased from Sigma-Aldrich. All the above chemicals were used as received. Deionized (DI) water was produced using a water purification system purchased from ELGA (Model: LA621).

2.2. Milling system

The milling system employed was a Retsch CryoMill operated at ambient conditions using plastic centrifuge tubes purchased from FisherBrand (2 mL, inner diameter 9 mm, length 40 mm) and milled with balls purchased from GlenMills (Hardened steel balls and alumina balls, 7/32″ in diameter). Steel ball and alumina balls weighs ~1.36 g and ~0.4 g, each respectively. All the experiments were conducted at room temperature (~25 °C). The frequency of milling varied from 3.0–25.0 Hz. And the milling period varied from 10 s to 99 min. In a typical experiment, 1 millimole of metal nitrate and the corresponding amount of potassium iodate were added to the 2-mL plastic centrifuge tube with 3 milling balls and milled at a frequency of 25.0 Hz (25/s) for 10 min. For example, 1 millimole of calcium nitrate tetrahydrate (molecular weight: 236.15) is 236.15 mg and the corresponding amount of potassium iodate (molecular weight: 214) is 2 millimole, or 428 mg. The theoretical product mass for calcium iodate (molecular weight: 408) is 408 mg. The three steel balls weigh 4.08 g and all reactants weigh 664.15 mg, thus the ball-to-powder mass ratio is 6.14. The temperature of the samples could in this period reach as high as ~318 K (45 °C) with hardened steel balls, and ~308 K (35 °C) with Al_2O_3 balls, as measured by a digital thermometer (Model: Hh11B, from Omega) just after milling.

2.3. Chemical precipitation method

For $Bi(IO_3)_3$, $Fe(IO_3)_3$and $AgIO_3$ synthesis, metal nitrate (0.044 mol/L) and potassium iodate (0.13 mol/L) aqueous solution were mixed dropwise to produce the precipitate (Fig. S1). However, using the same procedure, we could not get any $Ca(IO_3)_2$, $Mn(IO_3)_2$ and $Cu(IO_3)_2$ precipitate by this method initially. Crystal growth however does appear after ~24 h. The average size of the produced $Ca(IO_3)_2$, $Mn(IO_3)_2$ and $Cu(IO_3)_2$ crystals are ~1.7 mm, ~0.1 mm and ~0.4 mm (Fig. S2). To obtain smaller particles, the concentration of the three metal nitrates and potassium iodates used was increased to 1 mol/L and 0.3 mol/L, respectively. The precipitation reaction temperature and time were also elevated to 70 °C and 50 min in a water bath. The average size of the produced $Ca(IO_3)_2$, $Mn(IO_3)_2$ and $Cu(IO_3)_2$ crystals are ~100 μm, ~5 μm and ~2 μm (Fig. S3). The $Mn(IO_3)_2$ needles and $Cu(IO_3)_2$ plates also agglomerate into large spheres with a diameter of >20 μm and >10 μm, respectively. These needles and plates are not easy dispersed using ultra-sonication.

2.4. Washing/drying process

The product made by the above methods need to be processed by a simple washing and drying process. The samples were loaded into a large centrifuge tube (15 mL, FisherBrand) with 15 mL deionized water (DI water) and sonicated for 5 min, and centrifuged for 10 min at 7000 rpm (Labnet, Model: Hermle Z300) to obtain the final product. The whole process was repeated 3 times to enable full removal of any impurities. The sample was then dried overnight in a vacuum oven to remove free water. The final products were gently broken apart into powders with a spatula.

2.5. XRD, SEM/EDS, and TG/DSC

A Bruker X-ray diffractometer (XRD, D8 with Cu-kα radiation) was used to determine the crystallinity state of each metal iodate. A Hitachi Su-70 scanning electron microscope (SEM) attached with Energy-dispersive X-ray spectroscopy (EDS) was employed to analyze the particle size/morphology and elemental composition, respectively. The size of particles was directly measured from the SEM images by Nano Measurer 1.2. At least 200 particles for each sample were measured and the average reported. The metal iodate powders were attached to the SEM stage using carbon tape. A thin layer of Au (~3–5 nm) was deposited on the surface to increase the samples' conductivity before testing. Thermogravimetric/differential scanning calorimetry (TG/DSC) results were obtained with a TA Instruments Q600 at a rate of 10 °C/min up to 1000 °C in an argon atmosphere (100 mL/min).

3. Results and discussion

Generally, metal iodates precipitation can be obtained by mixing metal nitrate and potassium iodate solution as Eq. (1) shows. Table S1 shows the heat of formation of all the reactants and products and the Gibbs free energy change of each reaction. The latter is estimated as the change of reaction enthalpies (entropy change was assumed ~0). All the values of Gibbs free energy changes are negative, which means that based on Eq. (1), metal iodates form spontaneously.

$$M(NO_3)_x + xKIO_3 \rightarrow M(IO_3)_x + xKNO_3 \quad (1)$$

Six different metal iodates with cations spanning the periodic table from alkaline earth metals (such as Calcium) to transition metals (such as Iron) to post-transition metals (such as Bismuth) were synthesized by dry mechanochemistry and the corresponding SEM images in Fig. 1 shows a relatively narrow size distribution. For comparison, these metal iodates were also synthesized using a chemical precipitation method as shown in Fig. S1–S3. The details can be found in the

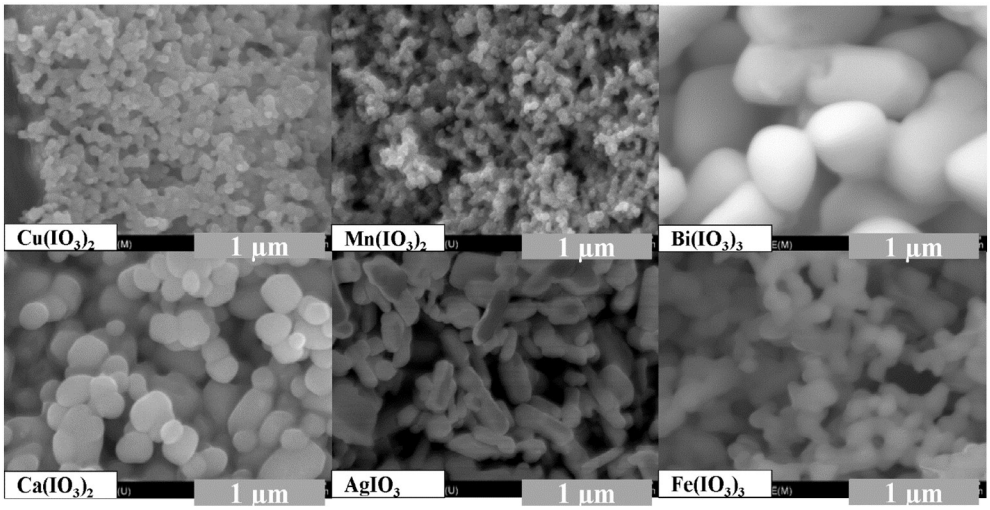

Fig. 1. SEM images of different metal iodates made by mechanochemistry. Note: both copper iodate ($3Cu(IO_3)_2 \cdot 2H_2O$) and calcium iodate ($Ca(IO_3)_2 \cdot H_2O$) have crystal water. Milling time = 10 min at 25 Hz.

Experimental section. Using chemical precipitation $AgIO_3$ can be prepared at room temperature. However, $Cu(IO_3)_2$, $Mn(IO_3)_2$ and $Ca(IO_3)_2$, typically required heating to 70 °C, for ~1 h. The resulting particles are quite large, with significant agglomeration (Fig S3).

Table 2 tabulates results for both ball milled and precipitation synthesis. Mechanochemistry produces much smaller sizes with narrower size distribution than precipitation growth. The average size of $AgIO_3$, $Cu(IO_3)_2$, $Mn(IO_3)_2$ and $Ca(IO_3)_2$ particles was reduced by a factor 20, 40, 100 and 500, respectively, when using mechanochemistry as compared to chemical precipitation. However, $Bi(IO_3)_3$ and $Fe(IO_3)_3$ mechanochemically generated particles were 6 and 3 times larger than those made from chemical precipitation, respectively. The latter result is presumably because the low solubility of $Bi(IO_3)_3$ and $Fe(IO_3)_3$ in water leads to a higher nucleation rate. Both $Bi(IO_3)_3$ and $Fe(IO_3)_3$ particles obtained by the chemical precipitation method are amorphous supporting this claim [31].

The XRD results of all the products after only 10 min's milling (25 Hz: milling frequency) are shown in Fig. 2 (except $Bi(IO_3)_3$ and $Fe(IO_3)_3$ cases) and clearly confirms that all the products are a mixture of metal iodates and the other by-product KNO_3, with no evidence of unreacted precursor. Washing (with water) is shown to leave only the desired metal iodate. (Fig. S4 and S5). The $Bi(IO_3)_3$ and $Fe(IO_3)_3$ cases are more complex which will be discussed later in this paper. The yields of metal iodates made by the two methods are also listed in Table 2. In general, the yields from the mechanochemical approach are >75%, and higher than chemical precipitation and in some cases, such as $Ca(IO_3)_2$ and $Cu(IO_3)_2$, the yield was almost doubled.

Table 2
Average size and yield of different metal iodates produced by chemical precipitation and mechanochemical method. Milling time = 10 min at a frequency of 25 Hz.

Materials	K_{sp}	Method	Average (nm)	Yield (%)
$Mn(IO_3)_2$	4.37×10^{-7}	Chemical precipitation	~5000	66.7
		Mechanochemistry	~50	75.7
$AgIO_3$	3.17×10^{-8}	Chemical precipitation	~3000	93.0
		Mechanochemistry	~150	96.2
$Ca(IO_3)_2 \cdot H_2O$	6.44×10^{-7}	Chemical precipitation	~100,000	35.8
		Mechanochemistry	~200	77.5
$3Cu(IO_3)_2 \cdot 2H_2O$	1.4×10^{-7}	Chemical precipitation	~2000	45.3
		Mechanochemistry	~50	81.7
$Bi(IO_3)_3$	–	Chemical precipitation	~130	83.7
		Mechanochemistry	~850	96.4
$Fe(IO_3)_3$	$\sim 10^{-14}$	Chemical precipitation	~50	80.3
		Mechanochemistry	~150	80.5

3.1. The role of thermal properties on the reaction

Generally, solid-solid reaction chemistry needs high pressure and/or high temperature for a sustained period to overcome the diffusion bottleneck for reaction. However, in this work, we achieve efficient reactions between solids at near ambient pressure and temperature. It is well accepted that the Tammann temperature (T_s) is a good metric to determine when atoms or molecules in a solid acquired sufficient energy for their bulk mobility and reactivity to become appreciable (such as to sinter) [39]. Therefore, the Tammann temperature is related to the melting point (T_m) of the solid. For example, the Tammann temperature for salts is usually evaluated as ~0.57 T_m (Kelvin scale) [39]. Table 3 shows the melting temperature, the calculated Tammann temperature and decomposition temperature (T_d) of various metal nitrates.

From Table 3, we see that all the hydrated metal salt except $Cu(NO_3)_2 \cdot 3H_2O$ have a low melting point <323 K (50 °C). This makes the corresponding Tammann temperature below 223 K (−50 °C). Direct measurement of temperature after 5 min of milling showed that the sample temperature was >318 K (45 °C) owing to the mechanical energy input, which is >100 K higher than the Tammann

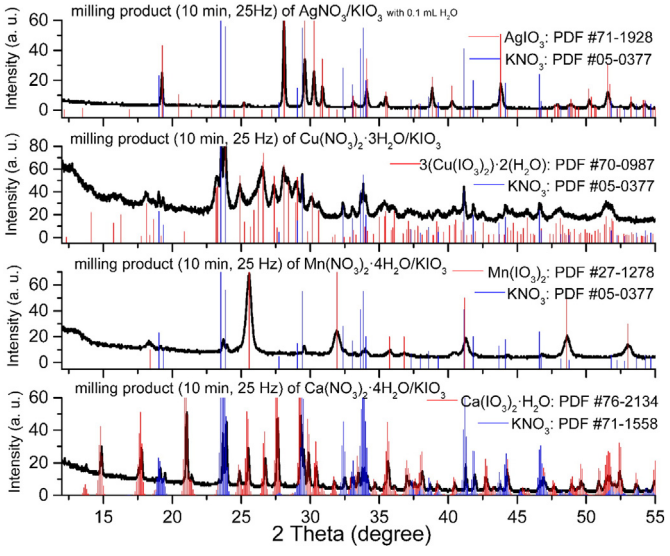

Fig. 2. XRD of ball milled products after 10 min milling (25 Hz).

Table 3
Melting and Tammann's temperature of various metal iodates.

Reactant 1	T_m, K	T_s, K	T_d, K	Obtained iodate by mechanochemistry?
$AgNO_3$	483	275	523–713	Yes with 0.1 mL DI water
$Bi(NO_3)_3 \cdot 5H_2O$	303	173	323–333	Yes with Al_2O_3 balls
$Cu(NO_3)_2 \cdot 3H_2O$	388	221	443	Yes
$Fe(NO_3)_3 \cdot 9H_2O$	320	182	398	Yes
$Mn(NO_3)_2 \cdot 4H_2O$	310	177	433–473	Yes
$Ca(NO_3)_2 \cdot 4H_2O$	316	180	–	Yes
KIO_3	833	475	833	–

temperature of the most metal nitrates. Therefore, according to the definition of Tammann temperature, the diffusion speed of mobile species into crystalline lattice should increase significantly when the temperature is higher than this critical point. Moreover, metal nitrates such as $Cu(NO_3)_2 \cdot 3H_2O$ are strongly hygroscopic which further promotes ion transport between the reactants. $AgNO_3$ and KIO_3 have a much higher melting point of 483 K and 833 K, raising their Tammann's temperatures as 275 K and 475 K, respectively.

The rapid reaction between metal nitrate and potassium iodate can be achieved mechanochemically, in part because the mechanical energy input will exothermically accelerate the ion diffusion after the temperature is raised above the Tammann temperature. To further confirm this, a simply mixed $Ca(NO_3)_2 \cdot 4H_2O/KIO_3$ and a ball milled product (25/s, 10 min) of $Ca(NO_3)_2 \cdot 4H_2O/KIO_3$ (both in stoichiometric ratio) were heated in a TG/DSC at 10 °C/min till to 1000 °C in argon. The simply mixed case was kept at ~50 °C for 30 min to complete the reaction. For a better comparison, all the reactants and products ($Ca(NO_3)_2 \cdot 4H_2O$, KIO_3, KNO_3 and $Ca(IO_3)_2 \cdot H_2O$) and a simply mixed $KNO_3/Ca(IO_3)_2 \cdot H_2O$ (same amount produced according to Eq. (1)) were also heated in the TG/DSC in the same procedure. As Fig. 3 shows, for the ball milled case, the TG/DSC curves are almost the same as that of $KNO_3/Ca(IO_3)_2 \cdot H_2O$, which indicates that the mechanochemical reaction is complete. For the simply mixed case, the TG/DSC curves are similar to that of the mixture of $KNO_3/Ca(IO_3)_2 \cdot H_2O$. That is, after being heated at 50 °C for 30 min, the simply mixed $Ca(NO_3)_2 \cdot 4H_2O/KIO_3$ has partially transformed to $KNO_3/Ca(IO_3)_2 \cdot H_2O$. One direct evidence is that the dehydration endothermic peak of $Ca(IO_3)_2 \cdot H_2O$ (~200 °C) and melting endothermic peak of KNO_3 (~330 °C) were all detected in the three curves. One interesting point is that there is a wide and deep endothermic peak around 50 °C for simply mixed $Ca(NO_3)_2 \cdot 4H_2O/KIO_3$ case while that peak for just $Ca(NO_3)_2 \cdot 4H_2O$ case is sharper. The shape change of this peak might be attributed to the reaction between $Ca(NO_3)_2 \cdot 4H_2O$ and KIO_3.

As we saw in Table 3, precursors at room temperature are already above the Tammann temperature in most cases. Simple mixing the two reactants of metal nitrates (except $AgNO_3$) with KIO_3 at room temperature will lead to interfacial reaction, however the reaction is limited by diffusion and thus milling is necessary to remove the reacted (product) interfacial layers to expose fresh material for continued reaction.

3.2. The role of hydration in the reaction

Fig. 4 shows, that the Tammann's temperature of $AgNO_3$ is as low as 275 K, however milling $AgNO_3$ and KIO_3 does not produce $AgIO_3$, which suggests the importance of crystal water. As shown in Table 3 and described above, $AgIO_3$ can be synthesized by milling with 0.1 mL DI water (Fig. 4). We note at this point that addition of 0.1 mL of water only dissolves a negligible amount of the two reactants, but should provide a pathway for ion transport.

To further explore the role of hydration in the diffusion and reaction, $Cu(NO_3)_2 \cdot 3H_2O$ and $Ca(NO_3)_2 \cdot 4H_2O$ were mixed with KIO_3 separately and characterized by SEM. In this experiment, the metal nitrate salts and KIO_3 crystals were freshly mixed before loading into the SEM without any other treatment. Fig. 5 shows that upon beam heating in the

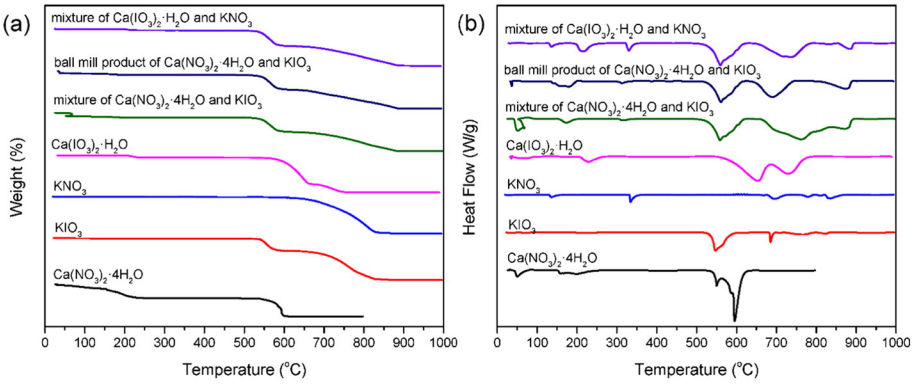

Fig. 3. TG and DSC results of different materials.

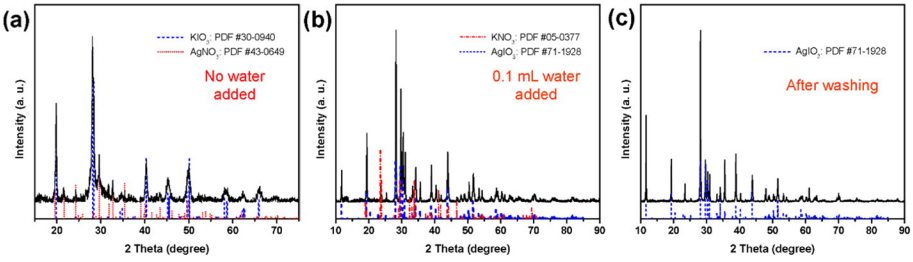

Fig. 4. XRD results of milling (25 Hz, 10 min) products of $AgNO_3/KIO_3$ (a), ball milling (25 Hz, 10 min) products of $AgNO_3/KIO_3$ (with 0.1 mL DI water, b), $AgIO_3$ (c) after 3 times washing with DI water of (b).

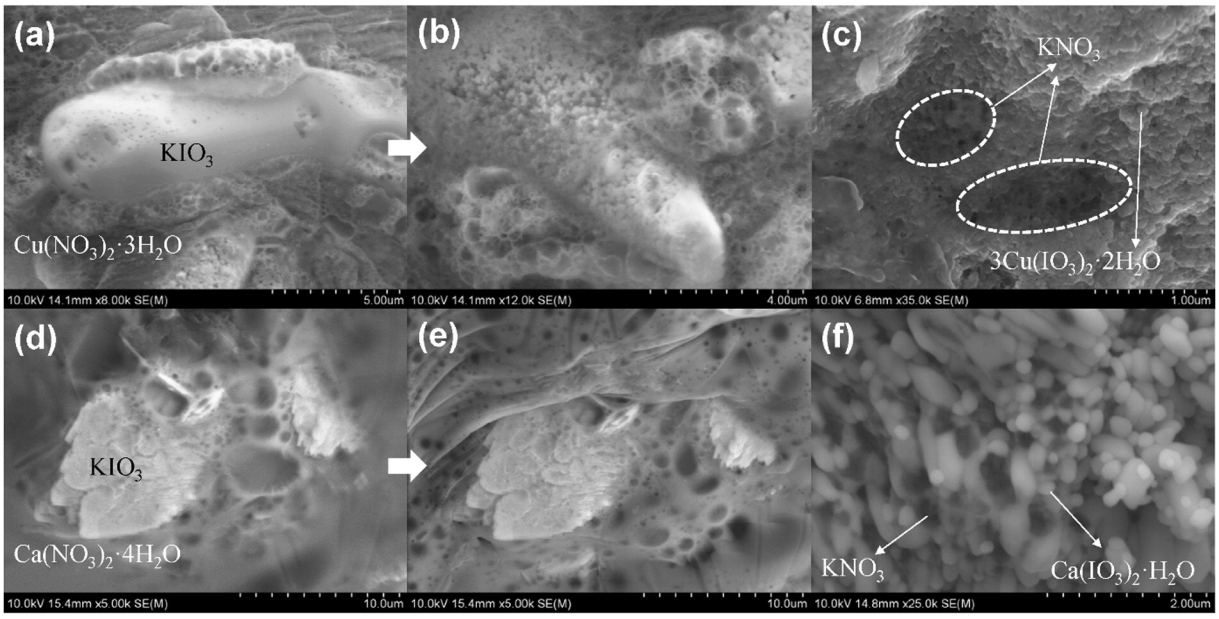

Fig. 5. SEM showing fast diffusion of KIO_3 into $Cu(NO_3)_2 \cdot 3H_2O$ (a and b) and $Ca(NO_3)_2 \cdot 4H_2O$ (d and e). The products after 10 min's milling of $Cu(NO_3)_2 \cdot 3H_2O/KIO_3$ mixture (c) and $Ca(NO_3)_2 \cdot 4H_2O/KIO_3$ mixture (f).

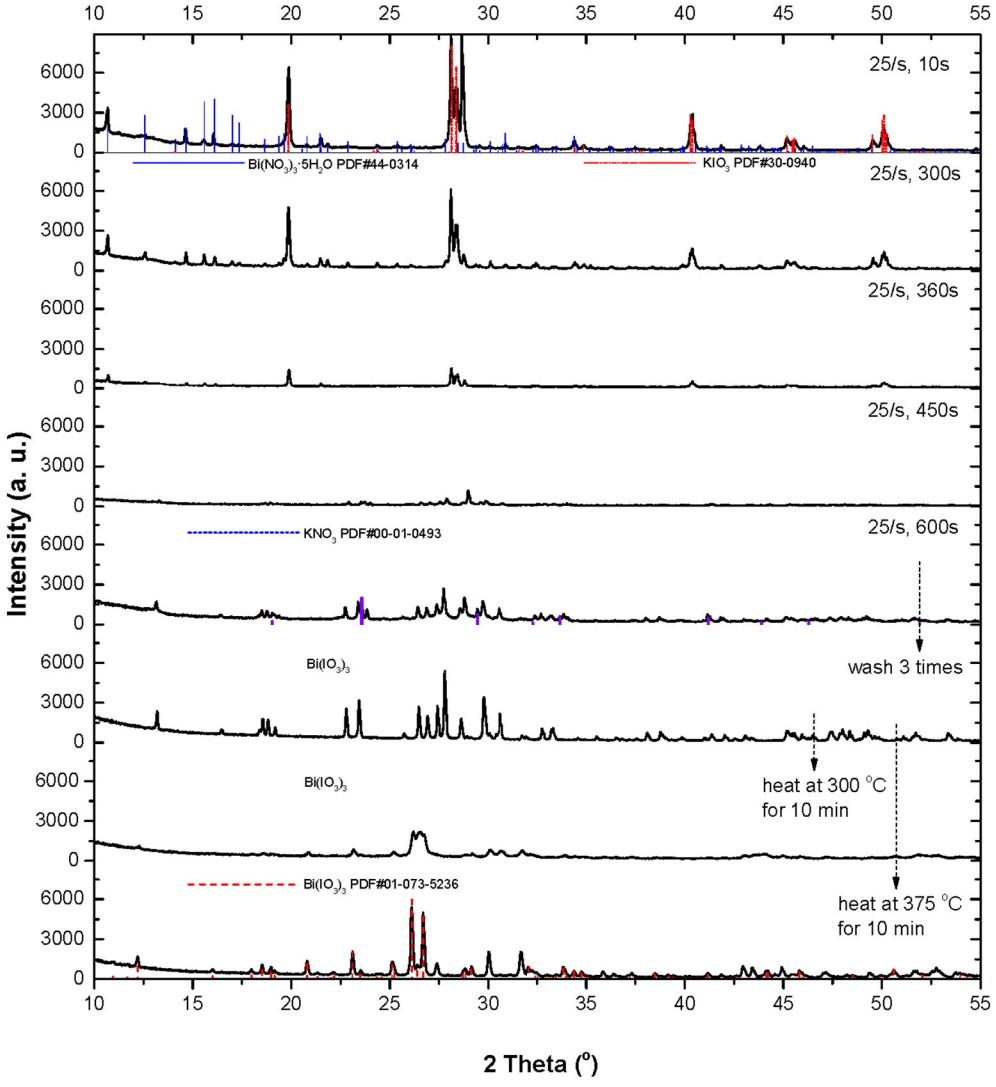

Fig. 6. Temporal XRD of milling $Bi(NO_3)_3 \cdot 5H_2O/KIO_3$ after 3 washings with DI water. Note: 25/s (25 Hz) is the frequency of shaking during ball milling.

SEM, the metal nitrates began to melt with bubbling, resulting from evaporation of water from nitrates. (confirmed by EDS) The spreading bubbles rapidly dissolved the exterior surface of KIO_3 crystals (Fig. 5a to Fig. 5b, Fig. 5d to e), which reacts to produce metal iodate NPs (confirmed by EDS) within a KNO_3 matrix. After washing away the KNO_3 (dark part in Fig. 5c and f), the monodisperse metal iodate NPs can be seen in Fig. 5f.

3.3. The role of milling time on the reaction

The milling products of $Bi(NO_3)_3 \cdot 5H_2O/KIO_3$, $Cu(NO_3)_2 \cdot 3H_2O/KIO_3$ and $Fe(NO_3)_3 \cdot 9H_2O/KIO_3$ with different milling durations and frequencies are shown in Fig. 6 and S5, respectively. Fig. 6 shows temporal XRD patterns of the effect of milling on $Bi(NO_3)_3 \cdot 5H_2O/KIO_3$. We note that Al_2O_3 balls were used instead of hardened steel balls (used for the others five metal iodates) in the synthesis of $Bi(IO_3)_3$. This is because the decomposition temperature of $Bi(NO_3)_3 \cdot 5H_2O$ is as low as 323–333 K. With hardened steel balls (~318 K), the temperature can temporarily reach the point of the decomposition of $Bi(NO_3)_3 \cdot 5H_2O$. And in fact, with hardened steel balls, Bi_2O_3 was detected in the final products, which confirms the above assumption. With Al_2O_3 balls, the temperature reached is only ~308 K, which is lower than the decomposition temperature (323 − 333 K) of the nitrate, but still much higher than its Tammann temperature (173 K). There is a decrease in $Bi(NO_3)_3 \cdot 5H_2O$ and KIO_3 intensity, with increased milling duration from 10 s to 360 s (25/s), which is essentially completely gone by 450 s. This decrease implies reaction is occurring, but the lack of any product diffraction pattern indicates an amorphous product or intermediate. New product diffraction patterns appear around 600 s which grow in intensity and decreases in peak width. This indicates that a nucleation process is over, and the remaining time results in crystallization and growth. After washing to remove the KNO_3 product, the final product, bismuth iodate is obtained (Fig. S6).

4. Discussion

Herein, we propose a possible mechanism involving the mechanochemical synthesis of metal iodate superfine powders. Upon milling, the reactant temperature is measured to increase rapidly to 318 K, which is >100 K higher than the Tammann temperature. This significantly enhances diffusion rates and reaction speed mediated by water as an ion conductor. The most interesting part of this work is that superfine metal iodates can be produced with a totally dry mechanochemical process with high efficiency (~600 s for a production of ~2500 mg). One key factor for the fast reaction is water (crystal water and free water) inside the metal nitrate salts. Metal nitrate salts with crystal water have a much lower Tammann temperature compared to those without crystal water. Most metal nitrate hydrates might contain some free water owing to their strong hygroscopic property, which further promotes the ion diffusion between the reactants. Milling attrits the particles to expose fresh unreacted surfaces and reduces particle size. Milling may also introduce defects [2] that contribute to the nucleation of the final products, in turn creating smaller particles. The continually formed KNO_3 may also act as a buffering material to protect metal iodates particles from decomposition and agglomeration.

5. Conclusions

In this work, we use a solid-solid mechanochemistry method to produce various metal iodate superfine powders. The formed particles have a much smaller and narrower size distribution compared to those made by the chemical precipitation method (except for $Fe(IO_3)_3$ and $Bi(IO_3)_3$). This method also has a high yield of >75% and a high production rate (2.5 g in 600 s), which is easily scalable. This method provides an economical and green approach for superfine powders synthesis.

Acknowledgment

This work was supported by Defense Threat Reduction Agency (DTRA). We acknowledge the support of the Maryland Nanocenter and its NispLab. The NispLab is supported in part by the NSF as a MRSEC Shared Experimental Facility.

Appendix A. Supplementary data

Supplementary data to this article can be found online at https://doi.org/10.1016/j.powtec.2017.10.024.

References

[1] P. Balaz, M. Achimovicova, M. Balaz, P. Billik, Z. Cherkezova-Zheleva, J.M. Criado, F. Delogu, E. Dutkova, E. Gaffet, F.J. Gotor, R. Kumar, I. Mitov, T. Rojac, M. Senna, A. Streletskii, K. Wieczorek-Ciurowa, Hallmarks of mechanochemistry: from nanoparticles to technology, Chem. Soc. Rev. 42 (2013) 7571–7637.
[2] S.L. James, C.J. Adams, C. Bolm, D. Braga, P. Collier, T. Friscic, F. Grepioni, K.D. Harris, G. Hyett, W. Jones, A. Krebs, J. Mack, L. Maini, A.G. Orpen, I.P. Parkin, W.C. Shearouse, J.W. Steed, D.C. Waddell, Mechanochemistry: opportunities for new and cleaner synthesis, Chem. Soc. Rev. 41 (2012) 413–447.
[3] S.L. James, T. Friščić, Mechanochemistry, Chem. Soc. Rev. 42 (2013) 7494.
[4] C. Xu, S. De, A.M. Balu, M. Ojeda, R. Luque, Mechanochemical synthesis of advanced nanomaterials for catalytic applications, Chem. Commun. 51 (2015) 6698–6713.
[5] M.A. Cambaz, M. Anji Reddy, B.P. Vinayan, R. Witte, A. Pohl, X. Mu, V.S.K. Chakravadhanula, C. Kübel, M. Fichtner, Mechanical milling assisted synthesis and electrochemical performance of high capacity $LiFeBO_3$ for lithium batteries, ACS Appl. Mater. Interfaces 8 (2016) 2166–2172.
[6] C. Suryanarayana, Mechanical alloying and milling, Prog. Mater. Sci. 46 (2001) 181–184.
[7] D.R. Weyna, T. Shattock, P. Vishweshwar, M.J. Zaworotko, Synthesis and structural characterization of cocrystals and pharmaceutical cocrystals: mechanochemistry vs slow evaporation from solution, Cryst. Growth Des. 9 (2009) 1106–1123.
[8] G. Wang, Mechanochemical organic synthesis, Chem. Soc. Rev. 42 (2013) 7668–7700.
[9] T. Friščić, D.G. Reid, I. Halasz, R.S. Stein, R.E. Dinnebier, M.J. Duer, Ion- and liquid-assisted grinding: improved mechanochemical synthesis of metal-organic frameworks reveals salt inclusion and anion templating, Angew. Chem. Int. Ed. 49 (2010) 712–715.
[10] T. Tsuzuki, P.G. McCormick, Mechanochemical synthesis of nanoparticles, J. Mater. Sci. 39 (2004) 5143–5146.
[11] G. Mi, Y. Murakami, D. Shindo, F. Saito, Mechanochemical synthesis of $CaTiO_3$ from a CaO-TiO_2 mixture and its HR-TEM observation, Powder Technol. 105 (1999) 162–166.
[12] V. Šepelák, I. Bergmann, A. Feldhoff, P. Heitjans, F. Krumeich, D. Menzel, F.J. Litterst, S.J. Campbell, K.D. Becker, Nanocrystalline nickel ferrite, $NiFe_2O_4$: mechanosynthesis, nonequilibrium cation distribution, canted spin arrangement, and magnetic behavior, J. Phys. Chem. C 111 (2007) 5026–5033.
[13] N.V. Kosova, N.F. Uvarov, E.T. Devyatkina, E.G. Avvakumov, Mechanochemical synthesis of $LiMn_2O_4$ cathode material for lithium batteries, Solid State Ionics 135 (2000) 107–114.
[14] F. Li, X. Yu, H. Pan, M. Wang, X. Xin, Syntheses of MO_2 (M = Si, Ce, Sn) nanoparticles by solid-state reactions at ambient temperature, Solid State Sci. 2 (2000) 767–772.
[15] T. Tsuzuki, K. Pethick, P.G. McCormick, Synthesis of $CaCO_3$ nanoparticles by mechanochemical processing, J. Nanopart. Res. 2 (2000) 375–380.
[16] S. Apperson, R.V. Shende, S. Subramanian, D. Tappmeyer, S. Gangopadhyay, Z. Chen, K. Gangopadhyay, P. Redner, S. Nicholich, D. Kapoor, Generation of fast propagating combustion and shock waves with copper oxide/aluminum nanothermite composites, Appl. Phys. Lett. 91 (2007) 243109.
[17] Z. Qiao, J. Shen, J. Wang, B. Huang, Z. Yang, G. Yang, K. Zhang, Fast deflagration to detonation transition of energetic material based on a quasi-core/shell structured nanothermite composite, Compos. Sci. Technol. 107 (2015) 113–119.
[18] H. Wang, G. Jian, G.C. Egan, M.R. Zachariah, Assembly and reactive properties of Al/CuO based nanothermite microparticles, Combust. Flame 161 (2014) 2203–2208.
[19] L. Wang, D. Luss, K.S. Martirosyan, The behavior of nanothermite reaction based on Bi_2O_3/Al, J. Appl. Phys. 110 (2011) 074311.
[20] R.A. Williams, J.V. Patel, A. Ermoline, M. Schoenitz, E.L. Dreizin, Correlation of optical emission and pressure generated upon ignition of fully-dense nanocomposite thermite powders, Combust. Flame 160 (2013) 734–741.
[21] H. Guan, C. Shao, B. Chen, J. Gong, X. Yang, A novel method for making CuO superfine fibres via an electrospinning technique, Inorg. Chem. Commun. 6 (2003) 1409–1411.
[22] J. Yu, B.W. McMahon, J.A. Boatz, S.L. Anderson, Aluminum nanoparticle production by acetonitrile-assisted milling: effects of liquid-vs vapor-phase milling and of milling method on particle size and surface chemistry, J. Phys. Chem. C 120 (2016) 19613–19629.
[23] S. Wang, M. Schoenitz, E.L. Dreizin, Mechanically alloyed magnesium–boron–iodine composite powders, J. Mater. Sci. 51 (2016) 3585–3591.
[24] T. Wakihara, A. Ihara, S. Inagaki, J. Tatami, K. Sato, K. Komeya, T. Meguro, Y. Kubota, A. Nakahira, Top-down tuning of nanosized ZSM-5 zeolite catalyst by bead milling and recrystallization, Cryst. Growth Des. 11 (2011) 5153–5158.

[25] M. Petrantoni, C. Rossi, L. Salvagnac, V. Conédéra, A. Estève, C. Tenailleau, P. Alphonse, Y.J. Chabal, Multilayered Al/CuO thermite formation by reactive magnetron sputtering: nano versus micro, J. Appl. Phys. 108 (2010) 084323.
[26] Z. Dong, J.F. Al-Sharab, B.H. Kear, S.D. Tse, Combined flame and electrodeposition synthesis of energetic coaxial tungsten-oxide/aluminum nanowire arrays, Nano Lett. 13 (2013) 4346–4350.
[27] J. Feng, G. Jian, Q. Liu, M.R. Zachariah, Passivated iodine pentoxide oxidizer for potential biocidal nanoenergetic applications, ACS Appl. Mater. Interfaces 5 (2013) 8875–8880.
[28] G. Jian, L. Liu, M.R. Zachariah, Facile aerosol route to hollow CuO spheres and its superior performance as an oxidizer in nanoenergetic gas generators, Adv. Funct. Mater. 23 (2013) 1341–1346.
[29] W. Zhou, J.B. DeLisio, X. Li, L. Liu, M.R. Zachariah, Persulfate salt as an oxidizer for biocidal energetic nano-thermites, J. Mater. Chem. A 3 (2015) 11838–11846.
[30] X. Hu, J.B. DeLisio, X. Li, W. Zhou, M.R. Zachariah, Direct deposit of highly reactive $Bi(IO_3)_3$-polyvinylidene fluoride biocidal energetic composite and its reactive properties, Adv. Eng. Mater. (2016)https://doi.org/10.1002/adem.201500532.
[31] H. Wang, G. Jian, W. Zhou, J.B. DeLisio, V.T. Lee, M.R. Zachariah, Metal iodate-based energetic composites and their combustion and biocidal performance, ACS Appl. Mater. Interfaces 7 (2015) 17363–17370.
[32] K.S. Martirosyan, L. Wang, A. Vicent, D. Luss, Synthesis and performance of bismuth trioxide nanoparticles for high energy gas generator use, Nanotechnol. 20 (2009) 405609.
[33] C.E. Johnson, K.T. Higa, Iodine-rich biocidal reactive materials, MRS Online Proc. Libr. 1521 (2013)https://doi.org/10.1557/opl.2013.46.
[34] J.C. Oxley, J.L. Smith, M.M. Porter, M.J. Yekel, J.A. Canaria, Potential biocides: iodine-producing pyrotechnics, Propellants Explos. Pyrotech. 8 (2017) 960–973.
[35] K.T. Sullivan, N.W. Piekiel, S. Chowdhury, C. Wu, M.R. Zachariah, C.E. Johnson, Ignition and combustion characteristics of nanoscale $Al/AgIO_3$: a potential energetic biocidal system, Combust. Sci. Technol. 3 (2010) 285–302.
[36] X. Hu, W. Zhou, X. Wang, T. Wu, J.B. Delisio, M.R. Zachariah, On-the-fly green generation and dispersion of AgI nanoparticles for cloud seeding nuclei, J. Nanopart. Res. 7 (2016) 214.
[37] S. Wang, X. Liu, M. Schoenitz, E.L. Dreizin, Nanocomposite thermites with calcium iodate oxidizer, Propellants Explos. Pyrotech. 3 (2017) 284–292.
[38] X. Liu, M. Schoenitz, E.L. Dreizin, Boron-based reactive materials with high concentrations of iodine as a biocidal additive, Chem. Eng. J. 325 (2017) 495–501.
[39] J.A. Moulijn, A.E. Van Diepen, F. Kapteijn, Catalyst deactivation: is it predictable? What to do? Appl. Catal., A. 212 (2001) 3–16.